JOURNAL OF CATALYSIS 128, 320–336 (1991)

An Investigation of Ethylene Hydrogenation Catalyzed by Metallic Molybdenum Using an Isolatable High-Pressure Reactor: Identification of the Reaction Site and the Role of Carbonaceous Deposits

LUPING WANG AND W. T. TYSOE[1]

Department of Chemistry and Laboratory for Surface Studies, University of Wisconsin, Milwaukee, Wisconsin 53211

Received July 3, 1990; revised November 6, 1990

Ethylene hydrogenation catalyzed by a model Mo(100) single crystal catalyst is investigated using an isolatable high-pressure reactor. The observed reaction kinetics are in agreement with those measured for supported transition metal hydrogenation catalysts showing a zero-order dependence in ethylene and a first-order dependence in hydrogen partial pressures. The reaction activation energy is 8.1 ± 0.5 kcal/mol for a Mo(100) single-crystal model catalyst and for a foil and mass spectral analysis of the products formed following substitution of deuterium for hydrogen shows that a maximum of two deuterium atoms are incorporated into the ethane that is produced. Auger analysis of the surface following reaction reveals the presence of large amounts of carbon (up to ~7 monolayers). This carbonaceous deposit decomposes on heating the surface to above 1000 K to desorb C_1 species. The experimental data suggest that either hydrogen or ethylene can permeate this layer so that hydrogen transfer takes place either at the metal surface or on top of the layer. Blocking the fourfold sites on Mo(100) by oxygen or carbon has only a marginal effect on the overall reaction kinetics, and does not substantially alter the amount of carbon deposited onto the surface during reaction. This result implies that the enhanced catalytic activity observed on metal carbide catalysts is not only due to site blocking, but also arises because of chemical modification of the catalyst by compound formation.

1. INTRODUCTION

The hydrogenation of small unsaturated hydrocarbons, and particularly ethylene, by transition metal catalysts has been the subject of considerable interest for many years, primarily since it is a model catalytic system which is particularly amenable to fundamental study. The reaction has been extensively studied over *supported* transition metal catalysts (*1–6*), and the problem has more recently been attacked using a combination of surface analysis techniques along with a detailed examination of the catalytic reaction under high pressure using the same single-crystal samples on which the surface analysis experiments were performed (*7*). Such studies have primarily focused on Group VIII transition metal-catalyzed reactions since these generally provide the most active and selective hydrogenation catalysts (*8*).

Detailed surface analysis has also revealed that chemisorbed ethylene rapidly transforms on these surfaces into an ethylidyne species at room temperature, for example on platinum (*9, 10*), rhodium (*11, 12*), and palladium (*13*). The catalytic role of the surface carbonaceous deposit, in this case consisting of ethylidyne, in ethylene hydrogenation has been probed by using an isolatable high-pressure reactor to carry out reactions using model single-crystal catalysts, where it was established that the Pt(111) single crystal surface provides a good model for a supported hydrogenation

[1] To whom correspondence should be addressed.

0021-9517/91 $3.00

catalyst (*7*). It was further proven, by synthesizing an ethylidyne layer incorporating radioactive ^{14}C, that the surface ethylidyne was present *during hydrogenation* and rehydrogenates at a rate much lower than that of the overall catalytic hydrogenation to form ethane (*14*). Thus, questions concerning the role of carbonaceous deposits in general, and ethylidyne in particular, in the hydrogenation reaction still remain. It has been postulated (*7*) that ethylidyne partially hydrogenates *to ethylidene* in the presence of a high pressure of hydrogen. The function of the ethylidyne in this case is to transfer hydrogen atoms from the metal surface to weakly adsorbed ethylene in the second layer. An alternative postulate holds that ethylidyne has *no* direct role in the reaction, but that this moiety is sufficiently mobile for the ethylene to gain access to the metal surface, and that hydrogenation proceeds between these surface ethylidyne groups (*15*).

Freshly prepared alumina-supported metallic molybdenum (Mo(0)) has been shown to be an extremely active hydrogenation catalyst (*16, 17*) and can be synthesized by decomposing $Mo(CO)_6$ supported on dehydroxylated alumina (*17–19*). More recently it has been shown that MoO_3 on alumina can be completely reduced to metallic molybdenum using rather severe conditions (*20*). Catalysts prepared via both routes (i.e., either starting from $Mo(CO)_6$ or MoO_3) exhibit identical catalytic properties (*21*) and, in particular, form extremely active alkene hydrogenation catalysts. Ethylene hydrogenation has also been studied on evaporated molybdenum films (*22, 23*), where the hydrogenation activity on molybdenum was found be significantly less than that on platinum, rhodium, nickel, and iron. It was also found that the extent to which the hydrogenation rate decreased as reaction proceeds was the largest on molybdenum.

It is shown in the following by experiments carried out in an isolatable high-pressure catalytic reactor using Mo(100) single crystals and high-purity molybdenum foils that metallic molybdenum catalyzes ethylene hydrogenation. Its activity (as measured from the turnover frequency) is *significantly* worse than both platinum and also freshly prepared supported Mo(0) but is in accord with the results on evaporated molybdenum films (*22, 23*). In addition, it is shown that a thick carbonaceous layer is detected on the surface using Auger spectroscopy following reaction. Such carbon deposition has been observed on supported, metallic molybdenum (*21*) and its role in hydrocarbon reactions has been scrutinized over a range of transition metals (*24–29*). The difference in hydrogenation activity between molybdenum and Group VIII metals and the presence of thick carbonaceous deposits is reflected in differences in their surface chemistries. Chemisorbed ethylene shows no tendency to form ethylidyne on Mo(100), and chemisorbed ethylene is almost completely decomposed into carbon, hydrogen, and smaller hydrocarbon fragments on annealing to room temperature (*30*). It is not surprising, therefore, that a thick carbonaceous layer forms on the surface during catalysis. However, in spite of the presence of a substantial amount of carbon on the surface, the model catalyst maintains a constant rate of hydrogenation over several thousand turnovers. In addition, the reaction kinetics (i.e., pressure dependencies and activation energies) measured for ethylene hydrogenation are typical for transition metal-catalyzed hydrogenation reactions (*1–8, 22*), being zero order in ethylene and first order in hydrogen pressures suggesting that similar mechanisms operate in all of these cases. Furthermore, substitution of deuterium for ethylene results in the incorporation of a maximum of two deuterium atoms in the ethane that is produced, suggesting that the reaction proceeds via a reaction pathway akin to that suggested by Horiuti (*31*).

Molybdenum carbide (Mo_2C), as well as carbides of tungsten and tantalum, has

been shown to provide an enhanced catalytic, and in particular, hydrogenation activity compared to the clean metal for a range of catalytic reactions (*32–39*). It is shown in the following that adsorbing a monolayer of carbon on molybdenum, in fact, slightly reduces (by ~20%) the activity for ethylene hydrogenation compared to the clean metal. A monolayer of adsorbed oxygen has a slightly larger inhibiting effect. Both of these adatoms adsorb at the fourfold site on Mo(100) (*40, 41*), suggesting that this site does not play an important role in the catalyzed hydrogenation reaction. In addition, no drastic modification of the amount of carbonaceous deposit is found by blocking the fourfold site with oxygen or carbon, indicating that the carbonaceous layer can also nucleate on other sites. These results imply that the formation of a compound and the resulting chemical modification of the catalyst plays an important role in the enhanced catalytic activity of carbides compared to metals.

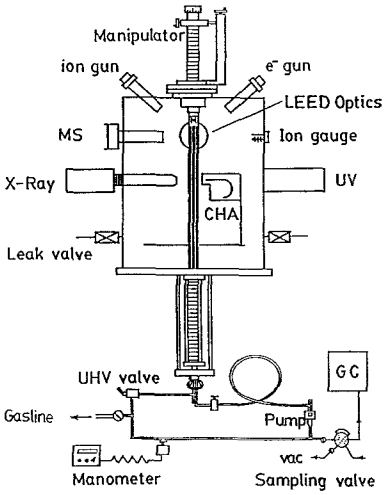

FIG. 1. Schematic diagram showing the isolatable high-pressure catalytic reactor incorporated into the ultrahigh vacuum apparatus. Shown also is the external recirculation loop.

2. METHODS

The experiments were carried out in an apparatus that has been described in previous publications (*42*). Briefly, however, the bakeable stainless-steel vacuum chamber is pumped by means of a liquid nitrogen-trapped diffusion pump and operates at a base pressure of 1×10^{-10} Torr (1 Torr = 133.3 N m^{-2}) following bakeout. The upper level of the chamber is equipped with an RFA for LEED and Auger spectroscopy measurements. It also contains a mass spectrometer for leak detection, residual gas analysis, and for thermal desorption spectroscopy. The ionizer of the mass spectrometer is in line of sight of and about 5 cm from the sample, which can be resistively heated. Heating rates of 30 K/s were used to obtain thermal desorption spectra.

The oriented Mo(100) single crystal is spot-welded to the end of a coaxial sample manipulator by means of tantalum wires, and temperatures are measured by means of a W 5%-Re/W 26%-Re thermocouple attached to the edge of the sample. The sample can be resistively heated to 2000 K and also can be cooled to 80 K via thermal contact to a liquid nitrogen-filled reservoir.

The apparatus also incorporates a coaxial isolatable high-pressure (up to ~1 atmosphere) catalytic reactor. A schematic diagram of the ultrahigh vacuum chamber and isolatable catalytic reactor is shown in Fig. 1. The reactor is closed by retracting the sample holder so that it rests on an anvil and the lower portion of the reactor is moved upward to completely enclose the sample. In order to facilitate rapid cell closure, the drive mechanism of the lower portion of the cell is motor driven, so that it takes approximately 40 s to move from fully retracted to fully closed. The cell is finally sealed by means of a thick, annealed copper gasket placed between the upper and lower parts of the cell. This arrangement seals sufficiently well that the pressure in the UHV apparatus is $\sim 5 \times 10^{-10}$ Torr with the cell filled to a pressure of 1 atmosphere. In addition, the internal surfaces of the reactor cell are gold

coated to minimize extraneous wall reactions. The reactor cell is connected to an external recirculation loop which is equipped with a capacitance manometer for pressure measurement, and a recirculation pump and sampling valve. The loop is also connected to a vacuum line for filling the cell and for evacuation after reaction. The total cell volume (i.e., reaction cell plus recirculation loop) is 108 ml, and the recirculation rate measured for air at 1 atmosphere pressure is 100 ml/min. After reaction, the cell typically takes 2–3 min to evacuate from 1 atmosphere to $\sim 1 \times 10^{-6}$ Torr. When the cell is opened to UHV at this pressure, a pressure burst of 5×10^{-9} Torr is typically observed in the main chamber, and, depending on which reactant gases are being used, the vacuum chamber typically takes ~ 1 min to pump to 5×10^{-10} Torr. Thus, the total time from high-pressure reaction conditions to UHV is generally less than 5 min. The cell operates as a batch reactor, and reaction rates are determined from product accumulation curves measured by analyzing reaction products using a gas chromatogram for conversions less than 1% in order to measure initial rates. In the case of the hydrogenation reactions described below, product concentrations are measured by diverting an aliquot of the reaction mixture to a gas chromatograph by means of a sampling loop (volume 0.2 ml). The gas chromatograph was equipped with a flame ionization detector and the $\frac{1}{8}$ in $\times$ 160 cm-long column was packed with Poropak N which was easily capable of separating ethylene from ethane. The nature of the reaction products is established from their retention times which are calibrated using gas mixtures of known composition. It is assumed in the kinetic analysis that the sensitivities of the flame ionization detector for ethylene and ethane are identical. The experimental protocol consisted of first sequentially introducing the required pressures of ethylene and hydrogen into the high-pressure cell. Finally, the total pressure in the cell was made up to 800 Torr using nitrogen, and the gas mixture was homogenized for 20 min using the recirculation pump. A sample of the reaction mixture was analyzed using the gas chromatogram prior to reaction to ensure that it contained no impurities, after which the sample was heated to the required reaction temperature. This time was taken as $t = 0$ for the reaction.

Two model catalyst samples were used for these experiments. The first was a Mo(100) single crystal that was prepared using standard metallographic techniques, and was oriented using X rays to within 0.5° of (100). A high-purity (99.995%) molybdenum foil was also used. This sample was attached directly to the sample support rods and the temperature was monitored by means of a W 5%-Re/W 26%-Re thermocouple spot-welded to the front face of the foil. In this case, the temperature indicated by the thermocouple was calibrated by means of an infrared pyrometer. Both samples were cleaned using a standard procedure which consisted of heating for several minutes to 1200 K in an ambient pressure of 2×10^{-7} Torr of oxygen and annealing several times *in vacuo* to 2000 K to remove oxygen (*43*). This procedure was repeated until no signals due to carbon or oxygen were detectable in Auger spectroscopy.

In order to ensure that ethylene hydrogenation is catalyzed by the molybdenum sample rather than the support wires, separate reactions were carried out using only the support wires, i.e., with the sample removed. In this case, the thermocouple was attached to the tantalum support wire which was heated to the temperatures used for ethylene hydrogenation with the crystal present.

The ethylene (Union Carbide, Linde; 99.6%) used for these experiments was transferred to a glass bulb, and vacuum distilled several times and stored in glass until use. The hydrogen (Airco; 99.999%) was used without further purification. A mass spectroscopic analysis of the reactant gases showed no impurities, in particular oxygen or water.

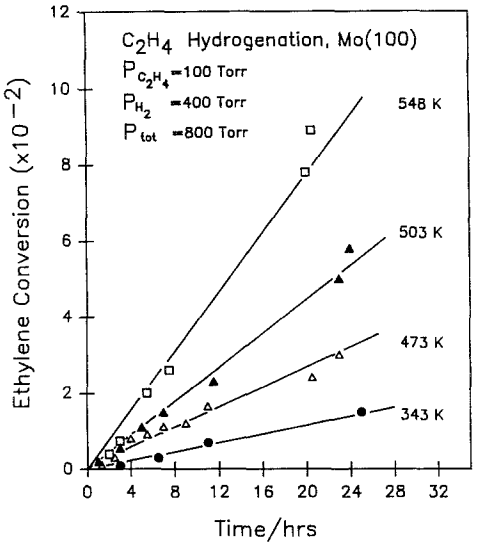

FIG. 2. Product accumulation curves for ethylene hydrogenation using an ethylene partial pressure of 100 Torr and a hydrogen partial pressure of 400 Torr, obtained using a Mo(100) model catalyst as a function of reaction temperature. Reaction temperatures are marked adjacent to their respective product accumulation curves.

3. RESULTS

The majority of experiments described below were carried out using an oriented Mo(100) single crystal. However, in order to check that the reaction was indeed catalyzed by the sample rather than on the reactor walls, another set of experiments were carried out using a polycrystalline molybdenum foil as model catalyst.

Measurement of the Kinetics of Ethylene Hydrogenation on Mo(100)

Hydrogenation reactions were carried out over a Mo(100) sample as a function of the sample temperature, and of both hydrogen and ethylene partial pressures. Resulting product accumulation curves are shown in Figs. 2 (as a function of temperature), 3 (as a function of hydrogen pressure), and 4 (as a function of ethylene pressure). Ethylene conversions were obtained by normalizing the ethane signal in the gas chromatogram to that of ethylene, and reaction rates were determined from the slopes of the product accumulation curves. For the cell volume and catalyst surface areas used for these experiments, a conversion of 1% corresponds to a total of $\sim 10^4$ reactions per surface site (where a surface site is taken to be a square unit cell on the Mo(100) surface, which has an area of 1×10^{-15} cm^2). As indicated in Figs. 2, 3, and 4, no induction periods were observed for any of the reactions. In all cases, reactions were followed up to total ethylene conversions of several percent, and the ethane formation rates remained constant over the whole conversion range. Blank reactions were also carried out in the absence of the single-crystal sample with the support wires heated to 548 K (the highest reaction temperature, Fig. 2) with a partial pressure of ethylene of 100 Torr and of hydrogen of 400 Torr. In this case, the rate of ethane formation was found to be $\sim 10\%$ of that with the single crystal present.

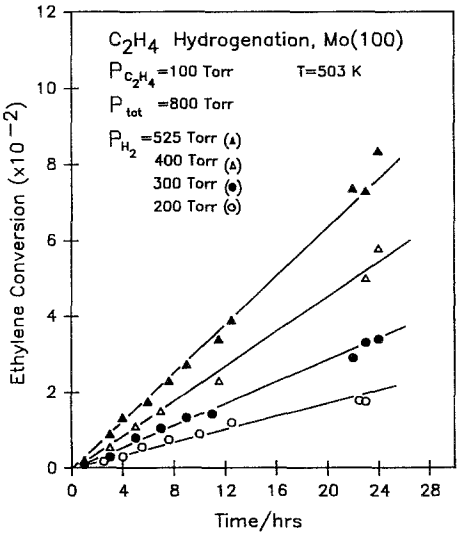

FIG. 3. Product accumulation curves for ethylene hydrogention using an ethylene partial pressure of 100 Torr and a reaction temperature of 503 K, obtained using a Mo(100) model catalyst as a function of hydrogen partial pressure, using hydrogen pressures of 200 (○), 300 (●), 400 (△), and 525 (▲) Torr.

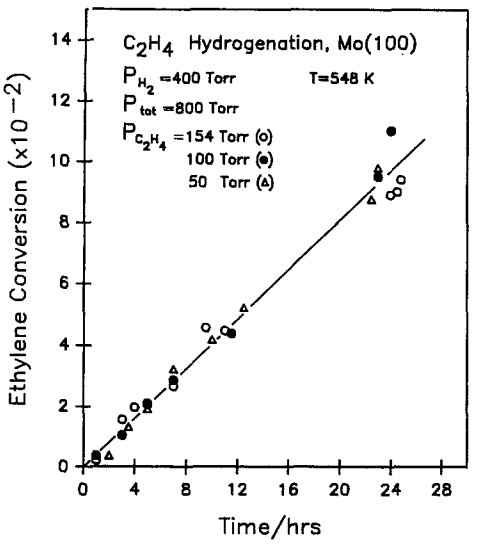

FIG. 4. Product accumulation curves for ethylene hydrogenation using a hydrogen partial pressure of 400 Torr and a reaction temperature of 548 K, obtained using a Mo(100) model catalyst as a function of ethylene partial pressure, using ethylene pressures of 50 (△), 100 (●), and 154 (○) Torr.

This indicates that a portion of the ethane found with the single crystal present must be ascribed to reaction on the tantalum support wires. This is, however, within the experimental error of the measured reaction rates. A similar experiment performed with the sample-support wires heated to 343 K (the lowest reaction temperature, Fig. 2) revealed *no* ethane formation within the detection limits of the gas chromatogram even after 24 h of reaction.

It is immediately clear (Fig. 4) that reaction rates are completely insensitive to ethylene partial pressures between 50 and 154 Torr, but show a significant dependence on hydrogen partial pressure (Fig. 3). Pressure dependencies are summarized in Fig. 5 as plots of $\log_{10}(N_t)$ versus $\log_{10}$ of both ethylene and hydrogen partial pressures, where N_t is the turnover frequency calculated for a crystal with an area of 0.54 cm^2 and assuming that a square unit cell on Mo(100) constitutes a reaction site. These results show that the reaction order with respect to the ethylene partial pressure is zero, and with respect to hydrogen partial pressure is 1.1 ± 0.1, that is, approximately first order in hydrogen partial pressure in good agreement with pressure dependencies measured on evaporated films (*22*). The temperature dependence of the reaction rate on Mo(100) is shown plotted in Arrhenius form (i.e., as $\ln(N_t)$ versus $1/T$) in Fig. 6, and the slope of this curve yields a reaction activation energy of 8.1 ± 0.5 kcal/mol. These kinetic results can be summarized in the following rate expression:

$$N_t = 3.4 \pm 0.5 \times 10^3 \; p(H_2)^{1.1 \pm 0.1} \; p(C_2H_4)^{0.0 \pm 0.1} \; \exp(-8.1 \pm 0.5 \times 10^3/RT)/\text{site/s},$$

where, as above, the number of surface sites is calculated assuming that a molybdenum surface unit cell on the (100) face constitutes a reaction site (and has an area of 1×10^{-15} cm^2), $p(H_2)$, and $p(C_2H_4)$ are the partial pressures of hydrogen and ethylene, respec-

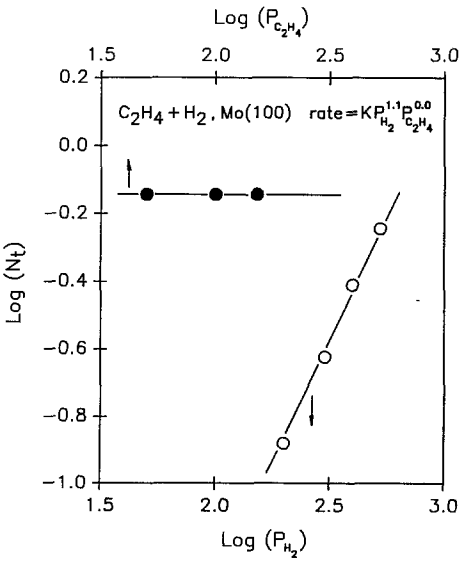

FIG. 5. Plot of $\log_{10}$ (reaction rate) (Log(N_t)) versus $\log_{10}$ (hydrogen pressure) (Log(P(H_2)); bottom axis, ○) and versus $\log_{10}$ (ethylene pressure) (Log(P(C_2H_4)); top axis, ●) showing the zero-order dependence in hydrogen partial pressure and the first-order dependence in ethylene partial pressure.

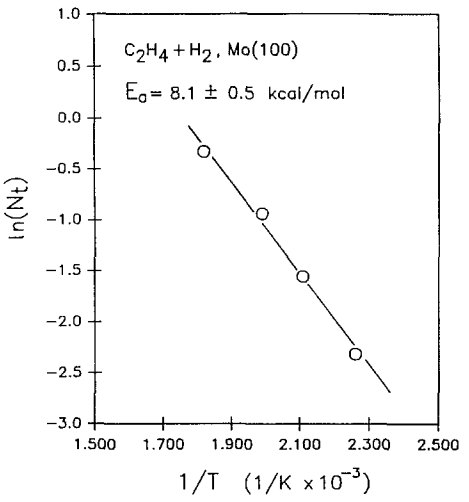

FIG. 6. The temperature dependence of ethylene hydrogenation catalyzed by a Mo(100) single crystal obtained using an ethylene partial pressure of 100 Torr and a hydrogen partial pressure of 400 Torr, plotted in Arrhenius form.

tively, measured in Torr, and T is the reaction temperature.

A reaction was carried out by substituting deuterium (100 Torr) for hydrogen, and by analyzing the product mass spectroscopically. This showed that the highest mass in the reaction products was at 32 amu, corresponding to the formation of $C_2H_4D_2$.

Measurement of Hydrogenation Kinetics on a Molybdenum Foil

A similar series of kinetic data were obtained for ethylene hydrogenation catalyzed by a molybdenum foil of exposed-faced area of 3.54 cm^2 using an exactly identical experimental protocol. The pressure dependencies are well reproduced for this sample showing an order in hydrogen pressure close to unity, and in ethylene pressure of zero. An Arrhenius plot for the hydrogenation reaction over molybdenum foil using a hydrogen pressure of 400 Torr and an ethylene pressure of 100 Torr (with the total pressure made up to 800 Torr using nitrogen) is shown in Fig. 7. The gradient of this curve yields an activation energy for ethylene hydrogenation of 8.1 ± 0.5 kcal/mol, a value in good agreement with that obtained using the oriented single crystal.

Analysis of the Surfaces after Reaction

The model catalyst surfaces were analyzed using Auger spectroscopy immediately after reaction, and the surfaces all exhibited substantial carbon contamination. Note that no oxygen contamination was detected on the model catalyst surface after reaction. The amount of carbon on the surface was determined from the ratio of the peak-to-peak amplitude of the C(KLL) Auger transition at 273 eV, ratioed to that of the peak-to-peak amplitude of the substrate molybdenum peak at 220 eV; designated C/Mo or I(C)/I(Mo). C/Mo ratios as large as 8 were measured. Shown in Fig. 8 is the C/Mo Auger ratio obtained following ethylene hydrogenation ($P(C_2H_4)$ = 100 Torr, $P(H_2)$ = 400 Torr) taken as a function of reaction temperature. Note that the Auger ratio varies significantly as a function of reaction temperature. The Auger ratio I(C)/

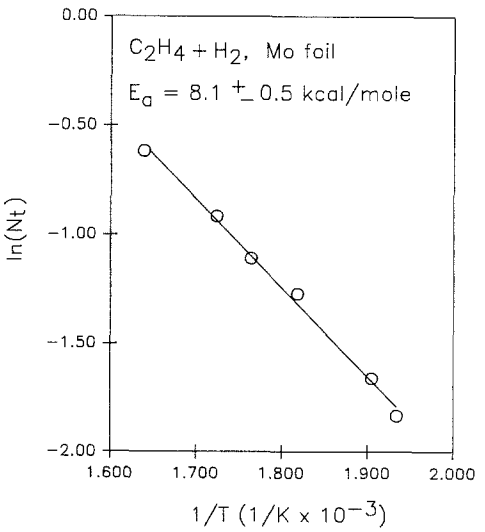

FIG. 7. The temperature dependence of ethylene hydrogenation catalyzed by a polycrystalline molybdenum foil obtained using an ethylene partial pressure of 100 Torr and a hydrogen partial pressure of 400 Torr plotted in Arrhenius form.

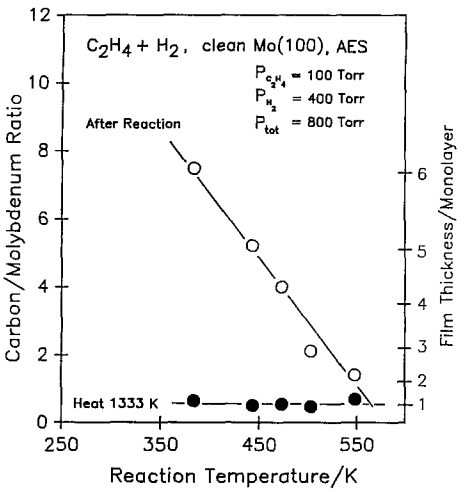

FIG. 8. Plot of the C/Mo Auger ratio for a Mo(100) single-crystal sample taken immediately following an ethylene hydrogenation reaction using an ethylene partial pressure of 100 Torr and a hydrogen partial pressure of 400 Torr taken as a function of reaction temperature (○). Shown also on the right-hand axis are film thicknesses estimated using the method outlined in the text. Also indicated (●) are the C/Mo ratios obtained by annealing the carbon-covered surface to 1333 K.

I(Mo) can be approximately related to the film thickness, t, through the formula

$$I(\mathrm{C})/I(\mathrm{Mo}) = \mathrm{C}[\exp(t/\lambda) - 1], \quad (1)$$

where λ is the electron mean free path in carbon. The value of λ can be estimated from the standard curve and is 3.5 monolayers (*44*), and the value of C calibrated from the value of I(C)/I(Mo) measured for a carbon layer of known thickness (i.e., 0.5 monolayers (*30*)). This procedure yields a value of C of 1.63. Resulting *estimates* of film thickness evaluated using this procedure have been plotted on the curves and show in Fig. 8 that up to approximately six monolayers of carbon are deposited onto the surface during reaction.

The amount of residual carbon at the surface following reaction was measured as a function of both ethylene and hydrogen partial pressures at a constant reaction temperature of 548 K. The results of these experiments are shown in Fig. 9 as a function of ethylene pressure and in Fig. 10 as a function of hydrogen pressure. These results indicate that the thickness of the residual carbon film is relatively insensitive to the partial pressure of hydrogen (Fig. 10) since the film thickness is constant between 3 and 4, whereas it *is* sensitive to the ethylene partial pressure, in particular for partial pressures up to 100 Torr (Fig. 9). Shown also plotted onto the graph of Figure 9 (of film thickness versus ethylene partial pressure) is a Langmuir function of the form

$$t = aP/(1 + bP), \quad (2)$$

where t is the film thickness, and P is the ethylene partial pressure in Torr, using values of 0.34 ± 0.07 for a and 0.1 ± 0.05 for b.

The thermal stability of these carbonaceous films was determined by measuring the C/Mo Auger ratio as a function of annealing temperature and the resulting values

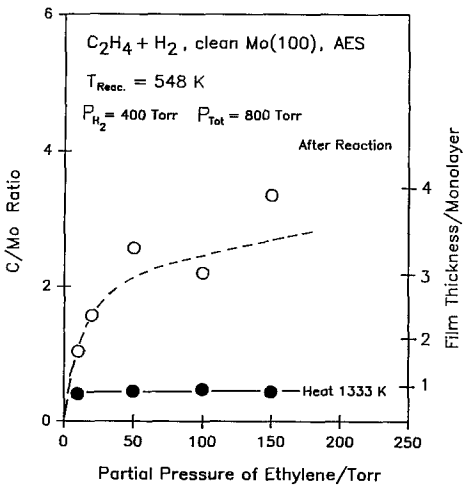

FIG. 9. Plot of the C/Mo Auger ratio immediately following an ethylene hydrogenation reaction using a reaction temperature of 548 K and a hydrogen partial pressure of 400 Torr taken as a function of reaction temperature (○). Superimposed on these data is a curve of the form $t = aP/(1 + bP)$. Shown also on the right-hand axis are film thicknesses estimated using the method outlined in the text. Also indicated (●) are the C/Mo ratios obtained by annealing the carbon-covered surface to 1333 K.

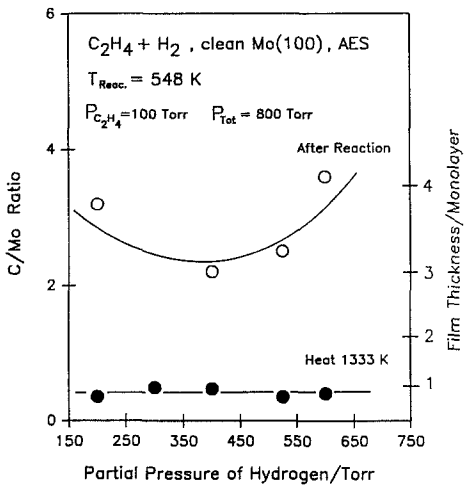

FIG. 10. Plot of the C/Mo Auger ratio immediately following an ethylene hydrogenation reaction using a reaction temperature of 548 K and an ethylene partial pressure of 100 Torr taken as a function of hydrogen pressure (○). Also indicated (●) are the C/Mo ratios obtained by annealing the carbon-covered surface to 1333 K. Shown also on the right-hand axis are film thicknesses estimated using the method outlined in the text.

of C/Mo Auger ratio are illustrated as a function of annealing temperature in Fig. 11. This shows that the carbon film thickness, t, remains constant up to an annealing temperature of ~800 K, and at ~1000 K the C/Mo Auger ratio (which corresponds to film thickness, t) decreases drastically to an approximately constant value after annealing to above 1300 K indicating a rapid depletion of surface carbon at this temperature. The final values of C/Mo Auger ratio measured after heating the surface to above 1333 K are also shown plotted on Figs. 8, 9, and 10 (●) following ethylene hydrogenation at various temperatures and reactant partial pressures. The final Auger ratio is always constant at 0.4 ± 0.1 irrespective of the original carbon layer thickness (i.e. reaction conditions) and corresponds to a carbon coverage $\theta(C) = 0.8 \pm 0.2$, or the presence of approximately one monolayer of carbon (*30*).

Attempts to rehydrogenate this surface carbonaceous layer in the high-pressure cell in the presence of 400 Torr of hydrogen at 550 K resulted in *no* diminution of the carbon Auger signal compared to the value before reaction. This indicates that the layer is completely stable to rehydrogenation under reaction conditions. This result is in accord with the observed relative insensitivity of the carbonaceous layer thickness as a function of hydrogen pressure.

The 2 amu (H_2) thermal desorption spectra of a Mo(100) single crystal covered with carbonaceous deposit following ethylene hydrogenation under various reaction conditions are shown in Fig. 12. All the spectra exhibit two peaks. The first is a broad peak between 700 and 900 K, and the other with somewhat variable position between 1100 and 1300 K. The peak temperature of the latter state corresponds well to the temperature at which the surface carbon coverage decreases on annealing (see Figs. 11 and 12). Peaks at this temperature were also detected when the mass spectrometer was tuned to 16, 14, and 12 amu, but *no* signal was detected at 27 amu. The relative desorption

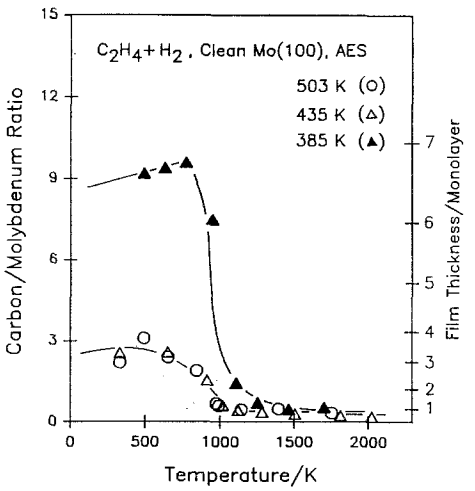

FIG. 11. Plot of C/Mo Auger ratio obtained as a function of annealing temperature for carbon-covered surface following ethylene hydrogenation using 400 Torr of hydrogen and 100 Torr of ethylene at temperatures of 503 K (○), 435 K (△), and 385 K (▲).

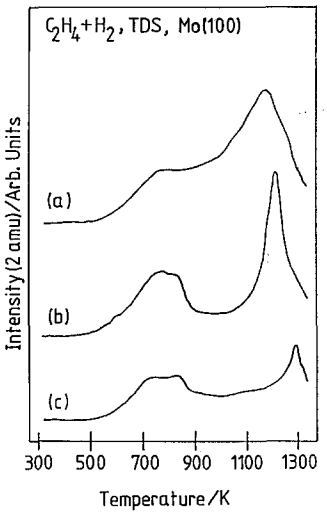

FIG. 12. 2 amu (H_2) thermal desorption spectra obtained from a Mo(100) single-crystal model catalyst using a heating rate of 30 K/s for surfaces covered with a carbonaceous layer following ethylene hydrogenation using 100 Torr of ethylene and 400 Torr of hydrogen at various reaction temperatures; (a) 540 K, (b) 380 K, (c) 360 K.

yields for these peaks are shown in Table 1, and compared with the relative intensities at these masses for methane using exactly identical mass spectrometer settings for both experiments. These results indicate that thermal decomposition of the carbonaceous layer produces C_1 hydrocarbons. The correspondence between the relative thermal desorption yields various masses and the mass spectrometer fragmentation pattern for methane is, however, no good. It should be mentioned that each of the thermal desorption spectra were collected after *different* catalytic reactions but under identical conditions, so that the reproducibility between spectra is not likely to be good. Another possible explanation for this discrepancy is that a portion of the carbonaceous layer can desorb as CH_2 fragments. Such CH_2 desorption from a hydrocarbon-covered molybdenum surface has been observed recently (*46*). The peak centered between 700 and 900 K shows no intensity in the 16, 14, and 12 amu spectra and is ascribed to the desorption of hydrogen.

TABLE 1

Comparison of the Mass Spectrometer Fragmentation Pattern for Methane with the Thermal Desorption Yield at Various Masses for the 1000 K Thermal Desorption State Obtained following Ethylene Hydrogenation

Mass	Thermal desorption yield	Methane mass spectrometer fragment intensity
27	0	0
16	100	100
14	62	16
12	68	2.5
2	—	0.2

Effect of Preadsorbed Carbon and Oxygen

Since metal carbides have been shown to be effective hydrogenation catalysts (*32–39*), a single crystal was covered by a monolayer of carbon (one carbon atom per substrate unit cell). In this case, carbon atoms occupy exclusively the fourfold hollow sites (*40*). The carbon-covered surface was obtained either by annealing the sample in 1×10^{-6} Torr of ethylene, or by heating a sample after reaction to 1300 K. Both of these procedures resulted in a carbon coverage, $\theta(C) = 1.0$, as determined using Auger spectroscopy. An oxygen-covered surface (also $\theta(O) = 1.0$) was also prepared for comparison. In this case, the oxygen was adsorbed by cooling the sample in 1×10^{-6} Torr of oxygen. This also results in the deposition of a monolayer of oxygen which occupies fourfold hollow sites (*41*).

Figure 13 displays the resulting product accumulation curves obtained when using these samples as hydrogenation catalysts at 623 K. The clean surface exhibits the highest reaction rate (0.28 reactions/site/s) with the rates for the carbon- and oxygen-covered surfaces being only slightly less, so that the turnover frequency for the carbon-covered surface is 0.23 reactions/site/s (lower by

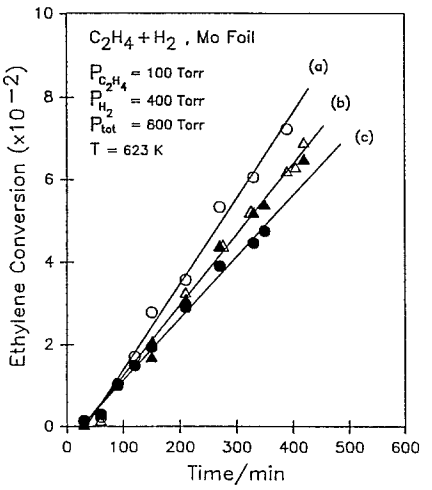

FIG. 13. Product accumulation curves obtained for ethylene hydrogenation using an ethylene partial pressure of 100 Torr, a hydrogen partial pressure of 400 Torr at a reaction temperature of 623 K for (a) clean molybdenum (○), (b) carbon-covered molybdenum obtained by cracking ethylene in UHV (▲), and by annealing a carbon-covered surface (△), (c) oxygen-covered molybdenum (●).

18%) and for the oxygen-covered surface is 0.22 (lower by 20%) (see Table 2). These reaction rates are normalized to the area of a surface unit cell on Mo(100) face which is taken to have an area of 1×10^{-15} cm^2. Note that the reaction rate is *exactly* identical for both carbon-covered surfaces irrespective of the origin of the carbon (i.e., whether it derives from annealing a surface following reaction of from ethylene decomposition) but slightly less than for the clean surface. The amount of carbon deposited on the surface during reaction as measured using Auger spectroscopy relative to the carbon layer thickness on the clean metal is also shown in Table 2, and indicates that carbonaceous layer formation is only slightly inhibited by preadsorbed carbon, but, in contrast, is accentuated by the preadsorbed oxygen.

4. DISCUSSION

The results of Figures 2, 3, and 4 show that a Mo(100) single crystal catalyzes the hydrogenation of ethylene to ethane at a constant rate over a wide range of experimental conditions, i.e., ethylene and hydrogen pressures and sample temperatures, up to conversions of ~10%. This conversion corresponds to a total number of turnovers per site in excess of $\sim 10^5$. Measurement of pressure dependences show that the reaction is close to zero order with respect to ethylene pressure, and approximately first order in hydrogen pressure (Fig. 5). The reaction activation energy measured on the Mo(100) single crystal is 8.1 ± 0.5 kcal/mole (Fig. 6) and on the foil is also 8.1 ± 0.5 kcal/mole (Fig. 7). The kinetic data for ethylene hydrogenation catalyzed by the Mo(100) single crystal are typical for this reaction over transition metal catalysts which predominantly show a first-order dependence in hydrogen pressure and a zero-order dependence in ethylene pressure (*8*) and, in particular, in good agreement with values obtained for evaporated molybdenum films (*22*).

TABLE 2

Comparison of the Relative Hydrogenation Rates of Molybdenum Covered by a Monolayer of Carbon or Oxygen with Initially Clean Molybdenum Model Catalysts

Catalyst	Turnover frequency (reactions/site/s)	Relative film thickness
Mo	0.28	1.00
Mo + 1 ml C(a)	0.23	0.88
Mo + 1 ml C(b)	0.23	0.91
Mo + 1 ml O	0.22	1.39

Note. (a) Sample prepared by annealing a sample covered with carbonaceous deposit; (b) sample prepared by cracking ethylene in UHV. Also, relative film thickness describes the thicknesses of the carbonaceous films formed following ethylene hydrogenation relative to that formed on the clean surface measured using Auger spectroscopy. Film thicknesses are estimated from the C/Mo Auger ratio using the method outlined in the text. Turnover frequencies are calculated by the ethane formation rate to the number of square unit cells on Mo(100) which have an area of 1×10^{-15} cm^2.

The reaction was carried out using both a molybdenum single crystal (with a surface area of 0.54 cm^2) and molybdenum foil (with surface area of 3.74 cm^2). For the molybdenum single crystal, the specific rate measured at a hydrogen partial pressure of 400 Torr and a partial ethylene pressure of 100 Torr for a reaction temperature of 548 K is 0.72 reactions/surface site/s. For the polycrystalline foil, using exactly identical reactant pressures (where the surface site area was taken to be identical to that on Mo(100)) the rate is 0.20 reactions/site/s at 551 K. The correspondence between these two rates which are within a factor of about 3 of each other, and which are normalized to the exposed surface areas of each of the samples, strongly suggests that the reaction is catalyzed by the molybdenum samples rather than, for example, on the reactor walls. Contributing factors to the differences between the reaction rates may be ascribed firstly to the assumption that the reaction site density on the foil and Mo(100) are identical at 1×10^{15} cm^{-2}, whereas the value on the polycrystalline foil is likely to be slightly different. In addition, the crystal is ~1 mm thick so that some reaction may be taking place on the edges of the sample. These results may also imply that the reaction is structure sensitive since the face of a polycrystalline sample is likely to exhibit a variety of crystal facets, and these results may explain the extremely high hydrogenation activity displayed by supported metallic molybdenum (*16, 17*). In addition, Auger analysis of the foil following reaction suggests that the carbonaceous deposits formed on the foils are somewhat thicker than those on the single crystal surface after identical catalytic experiments which might contribute to a slight lowering of the reaction rate. It should be mentioned that the foil sample was repeatedly heated to 2000 K during sample cleaning in order to remove surface oxygen arising from the carbon removal treatment. However, no LEED patterns were observed from the molybdenum foil which indicates that any surface order is less than ~100 Å, the coherence length of the electron beam. Finally, the agreement between activation energies measured for both samples over differing temperature ranges (Figs. 6 and 7) suggests that the reaction is not proceeding on the reactor walls since any wall heating is expected to be very different for each of the samples since they are considerably different in size. This result is in agreement with the experiments performed with no crystal present which showed a significantly lower rate of ethane formation than when the crystal is in place.

The specific rate for ethylene hydrogenation under the reaction conditions used in these experiments varied between ~1 and 0.1 reactions/site/s. This rate is significantly lower than measured for an alumina-supported metallic molybdenum catalyst (*16, 17*). The origin for this difference is not clear and may be due to electronic modifications due to the presence of small particles or perhaps an interaction with the support. It is clear from an Auger analysis of the surfaces following reaction that large coverages of carbonaceous deposit are present on the surface of the model catalyst (see Figs. 8, 9, and 10). Since the ethane formation rate is constant over a large number of turnovers (~10^5), it is likely that these films are at their equilibrium thicknesses, and the measured thicknesses represent a balance between their rate of formation, presumably by ethylene decomposition, and their rate of decomposition. The presence of a carbonaceous deposit appears to be a common feature in many hydrocarbon reactions, in particular over supported molybdenum and iron catalysts (*24–29*) and also, in the form of ethylidyne, on Group VIII surfaces (*7*).

Mass spectral analysis of the hydrocarbon products formed by reaction of ethylene ($p(C_2H_4)$ = 50 Torr) and deuterium ($p(D_2)$ = 400 Torr) at 540 K shows that the highest mass peak is at 32 amu, corresponding to the formation of $C_2H_4D_2$, indicating direct addition of deuterium to the ethylene. These results suggest the atomic hydrogen, presumably dissociated at the molybdenum

surface, adds to the ethylenic double bond according to the Horiuti–Polyanyi model [31], but in the presence of a thick layer of carbon. Questions still remain, therefore, concerning the site at which hydrogen is transferred to the adsorbed alkene, and the role (if any) of carbonaceous deposits in hydrocarbon catalysis. Two chemically distinct sites have been identified on Mo(100) single surfaces. The first is the fourfold hollow site, and the second is either the bridge or atop site. The differences between these sites is well illustrated by the chemistry of CO on molybdenum (*43*). The electronic structure of CO chemisorbed at the fourfold site on Mo(100) is modified to such an extent that the CO stretching frequency is lowered to ~1200 cm^{-1} (*45*). This CO is also tilted with respect to the surface allowing significant π-surface interaction and it rapidly dissociates into chemisorbed carbon and oxygen. In contrast, CO adsorbed at an atop site is significantly less modified, exhibiting a C–O stretching frequency of ~2100 cm^{-1} and which desorbs molecularly at ~300 K. This site displays a chemistry more closely akin to the less-reactive Group VIII metals. The reactivity pattern for CO is mirrored in the surface chemistry of ethylene on Mo(100) (*30*). In this case, ethylene adsorbs rapidly at the fourfold site, decomposing into carbon and hydrogen at somewhat above room temperature. In addition to this, a weakly bound ethylenic species is also detected which desorbs molecularly with an activation energy of between 7.5 and 9 kcal/mol depending on coverage. Clearly, since alkene hydrogenation is a rather mild catalytic process because it requires no alkene decomposition during reaction, alkene decomposition at any very reactive site will immediately block that site and passivate the surface, leaving only less reactive sites exposed. One role of the carbonaceous deposits appears, therefore, to be a site blocking agent. This view is substantiated since blocking the fourfold sites by either carbon or oxygen does not substantially affect the rate of hydrogenation (Fig. 12 and Table 2). These results also suggest that either bridge or atop sites are required for the reaction to proceed, at the very least for hydrogen dissociation. The carbonaceous layer thickness measured after ethylene hydrogenation at high pressure is, however, significantly larger than that required merely for site blocking. It is assumed in the following that metal (either bridge or atop) sites are required for the dissociation of hydrogen. There are several possibilities that can be envisaged for the way in which the subsequent reaction proceeds. The first is that the alkene can successfully permeate the hydrocarbon film and that hydrogen is transferred directly from the metal surface. Theoretical calculations do suggest that carbonaceous deposits in the form of an ethylidyne layer *are* sufficiently mobile to allow access of ethylene to a platinum surface (*15*). A second possibility is that hydrogenation can take place on top of the carbonaceous layer which is not permeable to the hydrocarbon. Hydrogen must then be transferred through the carbonaceous layer to the weakly adsorbed alkene on top of this layer. Note that thermal desorption spectra (Fig. 11) indicate that the carbonaceous layer does contain a significant amount of hydrogen. A final possibility is a combination of the two schemes outlined above. In this case, hydrogen dissociated at the surface is transferred to the carbonaceous layer, which is, in addition, permeable to alkene. Hydrogen is then transferred to the alkene from the carbonaceous layer which itself then effectively provides the sites at which the hydrogen is transferred. This last scheme can be immediately rejected based on the experimental evidence. The thickness of the carbonaceous layer increases as a function of ethylene pressure according to a Langmuir equation (Fig. 9 and Eq. (2)), so that if hydrogen is transferred from the surface to the carbonaceous layer and if this provides the site at which hydrogen is transferred to ethylene, the number of sites at which hydrogenation can occur should also vary in a manner similar to that of the carbonaceous layer

thickness. This would lead to a strong ethylene pressure dependence in the overall reaction rate, whereas the rate is, in fact, insensitive to ethylene pressure. In addition, the presence of a carbonaceous layer appears to *decrease* the overall reaction rate, also at variance with this model.

It is not possible, however, on the basis of the available experimental data to distinguish between the two remaining possibilities. It is clear, however, that catalytic hydrogenation requires the permeation of the carbonaceous layer by at least one of the reactants, either ethylene or hydrogen. This is undoubtedly a contributing factor to the lower activity of molybdenum as a hydrogenation catalyst than Group VIII metals. These results also suggest an intriguing possible alternative explanation for the insensitivity of reaction rate to ethylene pressure. This has been ascribed to a decrease in catalyst are available for reaction as a function of ethylene pressure (*1*). If permeation of the carbonaceous film by one of the reactants is a step in the reaction, and if the reaction is slowed by this process, it can be anticipated that the reaction rate will decrease with layer thickness. Thus, an increase in film thickness, which varies with ethylene pressure, will offset any increase in reaction rate due to an increase in ethylene coverage producing the observed insensitivity to ethylene pressure.

We focus now on the formation and nature of the carbonaceous layer. According to thermal desorption results (Fig. 11, Table 1), this carbonaceous layer can rapidly decompose on heating the surface to above 1000 K (Fig. 10) irrespective of the initial layer thickness. This suggests that the layer is of a rather uniform composition. The presence of a thermal desorption signal at 16 amu indicates that the carbonaceous film can decompose to desorb methane from the surface. However, the relative desorption yields at 12 and 14 amu do not correspond well to the mass spectrometer fragmentation pattern of methane (Table 2). It should be mentioned that each of the thermal spectra were obtained at the various masses after different catalytic reactions (since the mass spectrometer used for these experiments was not equipped with multimass capabilities), so that good reproducibility from spectrum to spectrum is unlikely. An alternative possibility for the discrepancy between the thermal desorption yields and the fragmentation pattern for methane is that the carbonaceous layer may also decompose to evolve CH_2 radicals. This phenomenon has been recently observed in hydrocarbon decomposition on molybdenum surfaces (*46*). No significant concentration of methane was detected in the reaction products suggesting that the rate of carbonaceous film decomposition is extremely slow compared to the overall alkene hydrogenation rate. This is not surprising in view of the high temperature required to thermally decompose the layer (>1000 K) compared to the reaction temperature.

Note that the thermal desorption spectra (Fig. 11) indicate that the carbonaceous layer incorporates significant amounts of hydrogen which might be available for alkene hydrogenation. The hydrogen desorption temperature in this case (~700 K) is significantly higher than that for hydrogen evolved from the first monolayer, either due to thermal decomposition of adsorbed hydrocarbon fragments (*30*) or due to hydrogen desorption from a clean (*47*) or carbon-covered surface (*48*). This indicates that this hydrogen desorption peak is associated with the carbonaceous layer. It is proposed that the layer is formed by ethylene decomposition at the metal surface, and that it decomposes to form methane (and perhaps methylene radicals) but appears not to be removed by reaction with hydrogen. The layer thickness is relatively insensitive to the hydrogen partial pressure (Fig. 9). This insensitivity to hydrogen partial pressure is in accord with the observation that the carbonaceous layer is not removed by heating to 540 K in the presence of 100 Torr of hydrogen in the high-pressure reactor.

The thickness of the resulting layer *does*,

however, depend strongly on ethylene partial pressure (Fig. 9), and the layer thickness depends on ethylene pressure, P, according to the equation, $t = bP/(1 + aP)$ and resembles a Langmuir isotherm in shape. The result is consistent with the view that the formation of the carbonaceous film is due to decomposition of chemisorbed ethylene which is in equilibrium with the gas-phase at the reaction temperature.

Blocking the fourfold site using either carbon or oxygen does not substantially alter the thickness of the resulting carbonaceous film. Based on the surface chemistry of ethylene on Mo(100) outlined above, it would be anticipated that the reactive fourfold site should provide the nucleus for the formation of the carbonaceous film. Clearly, however, the observation that blocking this site does not substantially alter the resulting carbonaceous film thickness implies that the carbonaceous layer can also be nucleated at other sites, i.e., either the bridge or atop sites, in the presence of high pressures of reactant. This observation is in accord with the view that the fourfold site is already blocked on the initially clean catalyst by alkene decomposition. Note also that there is some correlation between the rate of ethylene hydrogenation and the resulting carbonaceous layer thickness (Table 2) since the carbon-covered surface is more active than the oxygen-covered surface. However, the initially clean surface exhibits the highest overall catalytic rate, whereas the resulting carbonaceous layer thickness is intermediate between that on the carbon and oxygen-covered surfaces. These results imply that the enhanced activity of carbide catalysts compared to that of metals is not predominantly due to the blocking of very active sites to prevent carbonaceous layer formation (although this might play a role), but must also be ascribed to an electronic modification of the surface sites on the catalyst by compound formation which is likely, in particular, to significantly alter the electronic structure of the catalyst close to the Fermi level. It should be mentioned that substantial carbide formation is unlikely in the case of the model catalysts used here because of the extremely large bulk-to-surface ratio of both the foil and single-crystal model catalysts compared to supported metallic molybdenum.

Finally, although the reaction rate is not substantially effected by the presence of chemisorbed carbon or oxygen, there are slight differences between the observed rates for surfaces covered with these two adsorbates. These differences are larger than the experimental error in rate measurements since the data for two reactions carried out in the presence of carbon produced either by cracking an alkene in UHV or by annealing a carbon-covered surface following reaction can be superimposed (Fig. 12). This difference in rate for oxygen- and carbon-covered surfaces can be ascribed to various effects. First, as mentioned above, differences in rate between the carbon- and oxygen-covered surfaces may be due to differences in thickness of the resulting carbonaceous layers. The differences may also be due to an electronic modification of the surface by the presence of electronegative adsorbates. It has, for example, recently been shown that coadsorbed alkalis on Pt(111) can substantially effect the ethylene to ethylidyne transformation of chemisorbed ethylene (*49*). Another possible effect, since oxygen is slightly larger than carbon, is that chemisorbed oxygen may more effectively limit access to adjacent sites than chemisorbed carbon. This effect has been suggested previously (*50*).

5. CONCLUSIONS

The hydrogenation of ethylene has been investigated using an isolatable high-pressure catalytic batch reactor using a Mo(100) model single-crystal catalyst. The kinetic parameters (pressure dependences, activation energy) measured using this sample correspond well to those determined for supported metal hydrogenation catalysts and the product was found to incorporate a maximum of two deuterium atoms when substi-

tuting deuterium for hydrogen in the reaction. It was found, also, that hydrogenation proceeds in the presence of up to 6–7 monolayers of a carbonaceous deposit. The thickness of this deposit is found to depend strongly on both reaction temperature and ethylene partial pressure but to be insensitive to the partial pressure of hydrogen. Part of the role of the carbonaceous deposit is to block extremely active sites to prevent further hydrocarbon decomposition, and it is suggested that the reaction can proceed either directly on the metal surface, requiring the reactant alkene to permeate the carbonaceous layer, or alternatively on top of the carbonaceous layer requiring hydrogen diffusion through the layer.

Neither the hydrogenation rate nor carbonaceous layer formation is substantially effected by the presence of chemisorbed carbon or oxygen indicating that either atop or bridge sites can act as nucleation sites for carbonaceous layer formation. This suggests that compound formation and resulting electronic modification of surface sites is required to increase the hydrogenation activity in a carbide catalyst.

ACKNOWLEDGMENTS

We thank the donors of the Petroleum Research Fund, administered by the American Chemical Society, an Atlantic Richfield Foundation Grant of the Research Corporation and the University of Wisconsin—Milwaukee Graduate School for their support. One of us (L.P.W.) gratefully acknowledges receipt of a Research Fellowship from the Graduate School, and also the receipt of a Louise A. Arndt Fellowship. We thank Francisco Zaera for useful discussions and comments.

REFERENCES

1. Beeck, O., *Rev Mod. Phys.* **17,** 1 (1945).
2. Kemball, C., *J. Chem. Soc., Chem. Commun.,* 735 (1956).
3. Schuit, G. C. A., and Van Reijen, L. L., *in* "Advances in Catalysis" (D. D. Eley, W. G. Frankenburg, and V. I. Komarewsky, Eds.), Vol. 10, p. 298. Academic Press, New York, 1958.
4. Laidler, K. J., and Townsend, R. E., *Trans. Faraday Soc.* **57,** 1590 (1961).
5. Crawford, E., Roberts, M. W., and Kemball, C., *Trans. Faraday Soc.* **58,**1761 (1962).
6. Bond, G. C., Phillipson, J. J., Wells, P. B., and Winterbottom, J. H., *Trans. Faraday Soc.* **62,** 434 (1966).
7. Zaera, F., and Somorjai, G. A., *J. Amer. Chem. Soc.* **106,** 2288 (1984).
8. Bond, G. C., "Catalysis By Metals." Academic Press, New York, 1962.
9. Kesmodel, L. L., Dubois, L. H., and Somorjai, G. A., *J. Phys. Chem.* **70,** 2180 (1979).
10. Albert, M. R., Sneddon, L. G., Plummer, E. W., and Gustafson, T., *Surf. Sci.* **120,** 19 (1982).
11. Koestner, R. J., Van Hove, M. A., and Somorjai, G. A., *Surf. Sci.* **121,** 321 (1982).
12. Dubois, L. H., Castner, D. G., and Somorjai, G. A., *J. Chem. Phys.* **72,** 5234 (1981).
13. Minot, C., Van Hove, M. A., and Somorjai, G. A., *Surf. Sci.* **127,** 4411 (1982).
14. Davis, S. M., Zaera, F., Gordon, B. E., and Somorjai, G. A., *J. Catal.* **92,** 240 (1985).
15. Anderson, A. B., and Choe, S. J., *J. Phys. Chem.* **93,** 6145 (1989).
16. Bowman, R. G., and Burwell, R. L., Jr., *J. Catal.* **88,** 388 (1984).
17. Bowman, R. G., and Burwell, R. L., Jr., *J. Catal.* **63,** 463 (1980).
18. Nakamura, R., Pioch, D., Bowman, R. G., and Burwell, R. L., Jr., *J. Catal.* **93,** 388 (1985).
19. Nakamura, R., Bowman, R. G., and Burwell, R. L., Jr., *J. Amer. Chem. Soc.* **103,** 673 (1981).
20. Chung, J.-S., Zhang, J. P., and Burwell, R. L., Jr., *J. Catal.* **116,** 506 (1989).
21. Chung, J.-S., and Burwell, R. L., Jr., *J. Catal.* **116,** 519 (1989).
22. Kouskova, A., Adamek, J., and Ponec, V., *Collect. Czech. Chem. Commun.* **35,** 2538 (1970).
23. Merta, R., and Ponec, V., *in* "Proceedings, 4th International Congress on Catalysis, Moscow, 1968" (B. A. Kazansky, Ed.), p. 396. Adler, New York, 1968.
24. Briggs, D., Dewing, J., Barden, A. G., Moyes, R., and Wells, P. B., *J. Catal.* **65,** 31 (1980).
25. Páal, Z., Thomson, S. J., Webb, G., and McCorkindale, N. J., *Acta. Chim. Hungar.* **84,** 445 (1975).
26. Nakamura, J., Tanaka, K.-I., and Toyoshima, I., *J. Catal.* **108,** 55 (1987).
27. Hattori, T., and Burwell, R. L., Jr., *J. Phys. Chem.* **83,** 241 (1979).
28. Gupta, N. M., Kamble, V. S., and Iyer, R. M., *J. Catal.* **88,** 457 (1984).
29. Amariglio, A., and Amariglio, H., *J. Catal.* **78,** 44 (1982).
30. Wang, L. P., and Tysoe, W. T., *Surf. Sci.* **236,** 325 (1990).
31. Horiuti, J., *Catalyst* **2,** 1 (1948).
32. Sinfelt, J. H., and Yates, D. J. C., *Nature Phys. Sci.* **229,** 27 (1971).
33. Kojima, I., Miyazaki, E., Inoue, Y., and Yasumori, I., *J. Catal.* **59,** 472 (1979).
34. Boudart, M., Oyama, S. T., and Leclerq, L., *in*

"Proceedings, 7th International Congress on Catalysis, Tokyo, 1980" (T. Seiyama and K. Tanabe, Eds.), p. 578. Elsevier, Amsterdam, 1981.

35. Kojima, I., Miyazaki, E., Inoue, Y., and Yasumori, I., *J. Catal.* **73,** 128 (1982).
36. Leary, K. J., Michaels, J. N., and Stacey, A. M., *J. Catal.* **101,** 301 (1986).
37. Dun, J. N., Gulari, E., and Ng, K. Y. S., *Appl. Catal.* **15,** 247 (1985).
38. Yang, R. T., and Wong, C. J., *J. Catal.* **85,** 154 (1984).
39. Tsuchimoto, K., Suzuki, M., and Yamaki, M., *Nippon Kagaki Kaishi,* **10,** 1420 (1979).
40. Guillot, C., Riwan, R., and Lecante, J., *Surf. Sci.* **59,** 581 (1976).
41. Overbury, S. H., and Stair, P. C., *J. Vac. Sci. Technol.* **A1,** 1055 (1983d).
42. Wang, L. P., and Tysoe, W. T., *Surf. Sci.* **230,** 74 (1990).
43. Fulmer, J. P., Zaera, F., and Tysoe, W. T., *J. Chem. Phys.* **87,** 7265 (1987).
44. Seah, M. P., and Dench, W. A., *Surf. Interface Anal.* **1** (1979).
45. Zaera, F., Kollin, E., and Gland, J. L., *Chem. Phys. Letts.* **121,** 464 (1985).
46. Roberts, J. T., and Friend, C. M., *J. Amer. Chem. Soc.* **108,** 7204 (1986).
47. Han, H. R., and Schmidt, L. D., *J. Phys. Chem.* **75,** 227 (1971).
48. Ko, E. I., and Madix, R. J., *Surf. Sci.* **100,** L449 (1980).
40. Windham, R. G., Bartram, M. E., and Koel, B. E., *J. Phys. Chem.* **92,** 2862 (1988).
50. Deffeyes, J. E., Smith, A., and Stair, P. C., *Appl. Surf. Sci.* **26,** 517 (1986).